WEP Warwick Evans Publishing

International Journal of Public Health and Medical Research

ISSN: 3006-7707 (Print), ISSN: 3006-3752 (Online) | Volume 3, Number 3, Year 2025
DOI: https://doi.org/10.62051/ijphmr.v3n3.06
Journal homepage: https://wepub.org/index.php/IJPHMR/index

Optimization of Polishing Process of Ceramic Hip Joint Ball Spreading Method

Zihao Wei, Quanchao Jin

Tianjin University of Technology and Education, TianJin, China

ABSTRACT

This study takes the precision polishing process of small-diameter zirconia ceramic hip balls as the research object and focuses on exploring the mechanism of the abrasive particle movement trajectory on the surface quality. By establishing the three-dimensional motion trajectory model of the abrasive grains and the analytical model of the velocity field, based on the MATLAB numerical simulation platform, the influence laws of key parameters such as the initial position of the abrasive tool, the radius of the abrasive tool, the rotational speed ratio and the swing speed on the distribution characteristics of the abrasive grains were systematically analyzed, and the quantitative mapping relationship between the motion characteristic parameters of the abrasive grains and the surface roughness was constructed. On this basis, a surface quality control method based on multi-parameter collaborative optimization was proposed. The experimental verification results show that the polishing process parameters and system structure parameters significantly regulate the uniformity of material removal by influencing the spatial distribution characteristics of the abrasive particle movement trajectory. By optimizing the combination of parameters, the surface quality of spherical workpieces can be significantly improved.

KEYWORDS

Spreading method; Abrasive grain trajectory; Surface texture; Trajectory analysis

1. INTRODUCTION

Engineering ceramic materials, because of its unique microstructure, with high hardness, high strength, high temperature resistance, wear resistance, corrosion resistance, low density and high brittleness and other excellent properties, these characteristics make it in the machinery, electronics, chemical industry, military, aviation and other fields show a broad application prospects [1]. Among them, zirconia ceramics as an important class of engineering ceramic materials, in recent years has received widespread attention. With the continuous development of advanced manufacturing technology, precision zirconia ceramic parts and components have gradually realized the application of large-scale [2]. In zirconia ceramics precision machining, the core problem of the polishing process lies in the multi-scale coupling mechanism between abrasive grain trajectory and surface texture generation [3]. From the material removal mechanism analysis, mechanical polishing through the dynamic distribution of abrasive grain trajectory regulation of cutting, plowing and brittle fracture competition: trajectory coverage density determines the surface plastic deformation dominant zone and brittle fracture zone of the spatial distribution characteristics, directly affecting the uniformity of the distribution of the texture [4, 5]; abrasive tool movement path geometric topology characteristics of the trajectory directional superposition, constraints on the surface weaving of the evolution of the orientation of the law; and abrasive grain size The synergistic effect of abrasive grain size and load pressure dominates the gradient distribution of subsurface damage layer depth through the dynamic balance of trajectory energy transfer efficiency.

Li [6] Based on the improved isochord height error method to optimize the grinding trajectory of the overall bladed disk robot abrasive belt, the number of target points was reduced. Experiments verified that the processing efficiency increased by 42.9%, and the surface roughness Ra reached 0.26μm.

Wang [7] A grinding path optimization method based on the fragmentation of bone and joint surgical sites combined with genetic algorithm was proposed. Through the joint simulation verification of MATLAB and VREP, the degree of automation and surgical accuracy of orthopedic robots were significantly improved.

Zhang [8] Combining the Tian Niu must search with PID control to optimize the coordination of the four-wheel AGV steering motor, the deviation is corrected within 0.394 seconds under load disturbance, and the maximum fluctuation is reduced to 34.8%.Wang [9] The ultrasonic vibration-assisted polishing achieves material removal by generating a strong transverse shear flow to carry abrasive particles and impact the surface of the workpiece. The results show that the amount of material removed is positively correlated with the impact Angle of the abrasive particles. Fan [10] The parameters such as the processing gap and magnetic pole shape of magnetic grinding were analyzed by finite element using ANSYS Maxwell software, and the variation laws of the magnetic field and magnetic induction intensity were revealed through simulation. Ni [11] Based on the OpenFoam platform, the vertical entry process of three two-dimensional models of waterbird heads into water was simulated, and the characteristics of velocity, acceleration and trajectory were analyzed. The results show that the head shape and the speed of entering the water affect the asymmetric force causing deflection. At high speed, the smaller the J* value, the smaller the impact. Wang [12] The research involves defining coordinate transformation and structural parameters, constructing the circumferential tooth chip separation groove model, deriving the grinding trajectory using the coordinate transformation matrix, and verifying it through VC++ algorithm simulation to enhance the cutting performance and service life of the milling cutter.

At present, significant progress has been made in the research on the polishing of ceramic hip joint balls by the development method. However, due to the particularity of the sphere, the linear velocities of the sphere surface at different polishing positions vary, resulting in different densities of the polishing trajectory and further affecting the quality of the sphere surface. Furthermore, when the spherical surface forms a fixed Angle with the grinding tool for polishing, systematic errors result in a smaller number of abrasive grains passing through the vertex position of the ball, thereby affecting the polishing effect. In addition, the size of the grinding tool radius also affects the trajectory pattern on the ball surface during the polishing process. Therefore, this paper focuses on studying the coupling mechanism between the abrasive particle movement trajectory and the surface morphology during the polishing process of zirconia ceramic spheres with small-diameter grinding tools. By constructing a three-dimensional kinematic model of abrasive grains, the action path of trajectory distribution on surface quality is clarified. This study will analyze the regulation laws of polishing process parameters (such as initial position, radius, and rotational speed ratio) on the grinding mark trajectory based on the spatial trajectory equation and the inversion method. Further, the fixed step size analysis method and Voronoi diagram analysis method were adopted for texture analysis. Eventually, a surface topography control framework with trajectory optimization as the core was established, and the correlation between trajectory parameters and surface functional characteristics was verified through experiments.

2. THE PROCESSING PRINCIPLE OF CERAMIC SPHERICAL SURFACES BY THE DEVELOPMENT METHOD

The principle of processing ceramic spherical surfaces by the development method is based on the theory of envelope forming [13, 14], As shown in Figure 1, its core is to make the movement trajectory of the tool surface spatially envelope the target spherical surface through the relative motion between the tool and the workpiece. From a geometric perspective, any cross-section of a sphere is a planar circle, and any planar circle can intersect with a sphere whose diameter is no less than that of itself, forming a spatial curve of the same length as the circumference of the plane. When the axis of a sphere intersects the axis of a plane circle at a specific Angle and rotates around the intersection point, the trajectory of the plane circle will envelope to form a complete spherical surface, and the intersection point is the center of the sphere. Based on this geometric principle, during the spherical grinding process, by adjusting the axis of the workpiece and the axis of the grinding wheel to a specific Angle and rotating them respectively around their respective axes, the relative motion trajectories of the grinding wheel and the workpiece meet the envelope conditions, thereby precisely forming the target spherical surface.

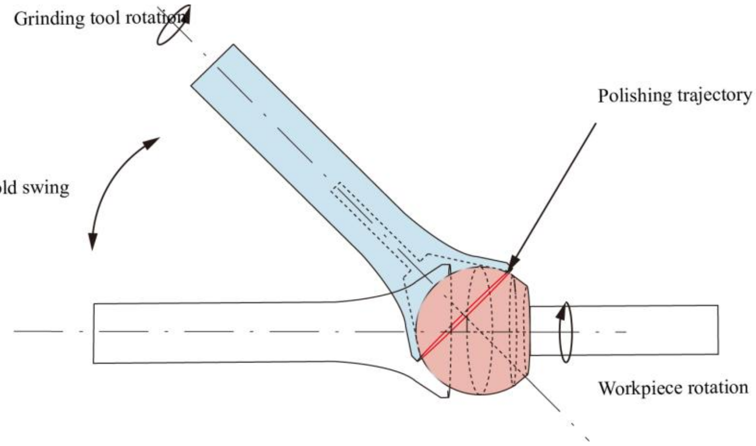

Figure 1. The processing principle of the development method

During the polishing process, the electric spindle drives the pad below through the slider installed on the linear ball screw to achieve linear motion. The cup-shaped grinding tool is installed on the ultrasonic tool holder, which is fixed on the electric spindle. Meanwhile, an ultrasonic generator is installed at the end of the spindle. When the main shaft rotates, it drives the tool holder and the grinding tool to rotate along their own axes. The other one end of the motor is equipped with a special ceramic ball fixture and is connected to the roller bearing through bolts, enabling it to rotate by itself as well as achieve rotary motion. The entire polishing device relies on two motors to provide rotational motion, while roller bearings provide rotary motion, making the axes of the three movements converge at one point. The movement of the electric spindle is precisely controlled by the ball screw to adjust the feed accuracy of the cup-shaped mold and conduct force feedback detection, thereby achieving precise polishing of the ceramic balls, as shown in Figure 2.

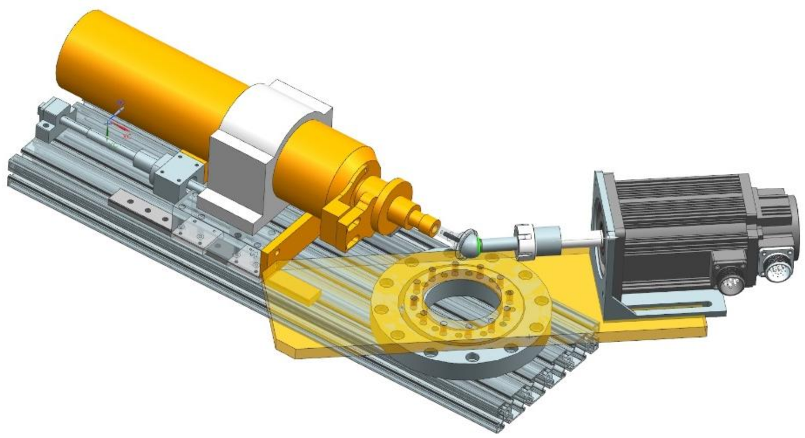

Figure 2. Device processing drawing

3. ESTABLISHMENT OF THE MATHEMATICAL MODEL OF ABRASIVE PARTICLE TRAJECTORIES

During the polishing process of ceramic balls, the surface trajectory movement is comprehensively influenced by multiple key factors, among which the most significant ones are the rotational movement of the workpiece around the spindle, the self-rotation movement of the grinding wheel around the grinding wheel shaft, and the swinging of the grinding tool. These movements interact with each other, determining the shape, distribution and uniformity of the surface trajectory.

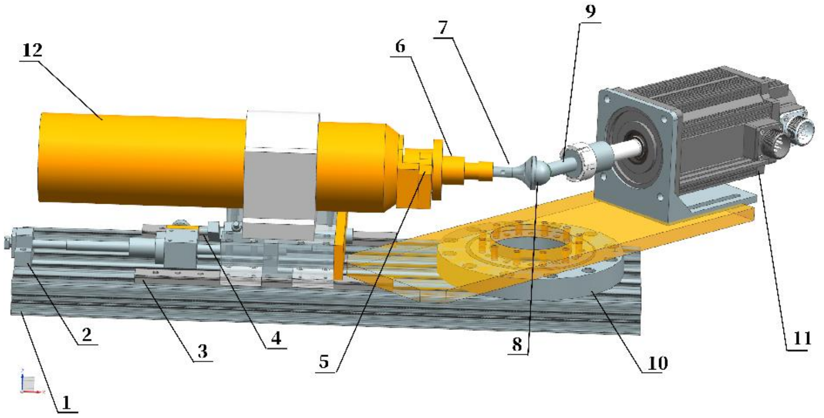

Figure 3. 1- Workbench, 2- Ball screw, 3- Linear guide, 4- Force gauge, 5- Ultrasonic generating device, 6- Ultrasonic tool holder, 7- Cup-shaped grinding tool, 8- Ceramic ball, 9- Fixture, 10- Crossed roller bearing, 11- Servo motor, 12- Water-cooled spindle

Grinding marks refer to the processing traces left by abrasive grains during their movement on the surface of a workpiece. Their shape and distribution directly affect the surface quality, roughness and final performance of the workpiece. In order to accurately describe and solve the parametric equation of the abrasive particle trajectory, the inversion method and the matrix equation method need to be adopted, that is, to convert the coordinate system to the workpiece itself, so as to analyze the motion characteristics of the abrasive particles on the workpiece surface more clearly. In this method, taking the center of the workpiece sphere as the coordinate origin, the workpiece coordinate system O-xyz is established, thereby simplifying the trajectory calculation and providing a theoretical basis for further optimizing the polishing process.

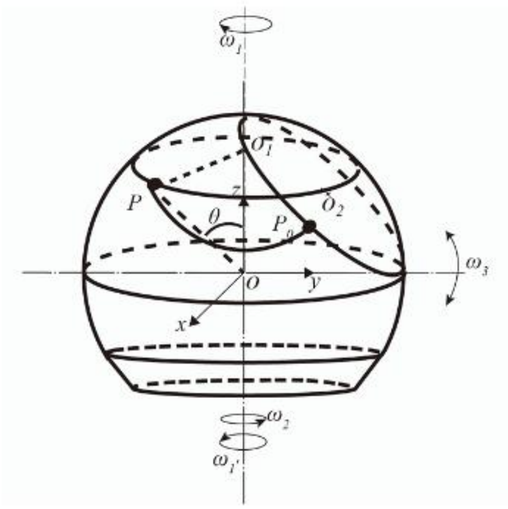

Figure 4. Schematic diagram of the relative motion between abrasive grains and workpieces

3.1. Establishment of the Abrasive Particle Trajectory Motion Model

When conducting mathematical modeling of the movement trajectory of abrasive grains on the ball surface, it is necessary to first analyze the movement of the abrasive grains on the ball surface. Assuming that relative motion is being carried out, the conical surface of the grinding tool is in full contact with the surface of the ball head and the movement center has not shifted, and the feed speed of the grinding tool in the feed direction of the main shaft is fixed and not affected by vibration, then this abrasive grain mainly contains three movements during the polishing process: The rotational speed of the cup-shaped grinding tool around its axis is ω_1, the rotational speed of the ceramic ball is ω_2, and the pendulum speed of the ceramic ball itself is ω_3. However, since it is a relative motion, the subsequent trajectory diagram and motion formula are all based on the grinding tool as the swing reference. Among them, the rotation center of the ceramic ball is O_1, The radius is R, The distance between the abrasive grains and the rotational axis of the grinding tool is r (grinding tool radius), The center of the contact circle between the grinding tool and the ceramic ball is O_2 (the center of the grinding tool), The distance between O_1 and O_2 is L. Suppose a certain abrasive grain on the grinding tool comes into contact with the ceramic ball at $t = 0$, Its coordinate is $P(x_0, y_0, z_0)$, When time t passes, the abrasive particles move from $P(x_0, y_0, z_0)$ to $P_0(x_1, y_1, z_1)$.

The spatial position of the abrasive particles at time t is calculated by the inversion method and the spatial matrix method as:

$$\begin{cases} x_3 = r\cos(w_1 t)\cos(w_2 t) - \left[r\sin(w_1 t)\cos(\theta_0 \sin(w_3 t)) - r\cos\theta \sin(\theta_0 \sin(w_3 t))\right]\sin(w_2 t) \\ y_3 = r\cos(w_1 t)\sin(w_2 t) + \left[r\sin(w_1 t)\cos(\theta_0 \sin(w_3 t)) - r\cos\theta \sin(\theta_0 \sin(w_3 t))\right]\cos(w_2 t) \\ z_3 = r\sin(w_1 t)\sin(\theta_0 \sin(w_3 t)) + r\cos\theta\cos(\theta_0 \sin(w_3 t)) \end{cases} \quad (1)$$

The above is the trajectory motion expression of a single abrasive particle. In the actual polishing process, there are countless abrasive particles on the surface of the ceramic ball performing polishing, but the trajectory equations between different abrasive particles only differ by a certain phase Angle. According to the formula, the

trajectory of the i-th abrasive particle can be obtained as:

$$\begin{cases} x_i'(t) = r\cos(w_1 t + \phi_i)\cos(w_2 t) - \left[r\sin(w_1 t + \phi_i)\cos(\theta_0 \sin(w_3 t)) - r\cos\theta \sin(\theta_0 \sin(w_3 t))\right]\sin(w_2 t) \\ y_i'(t) = r\cos(w_1 t + \phi_i)\sin(w_2 t) + \left[r\sin(w_1 t + \phi_i)\cos(\theta_0 \sin(w_3 t)) - r\cos\theta \sin(\theta_0 \sin(w_3 t))\right]\cos(w_2 t) \\ z_i'(t) = r\sin(w_1 t + \phi_i)\sin(\theta_0 \sin(w_3 t)) + r\cos\theta\cos(\theta_0 \sin(w_3 t)) \end{cases} \quad (2)$$

Through the above formula, the movement trajectory of each abrasive particle can be represented by a unified formula, and the difference in the initial position is described by ϕ_i to ensure that the abrasive particles are uniformly distributed on the contact circle.

3.2. Establishment of Abrasive Particle Trajectory Velocity Model

Although the classic constant-speed swing mode can ensure the stability of motion, it is difficult to overcome the distortion of the velocity field caused by spherical curvature. When the grinding tool swings at a fixed angular velocity, the area near the pole has a sharp attenuation of the linear velocity at the contact point, and its relative velocity is much smaller than the linear velocity in the equatorial area. This geometric non-uniformity leads to significant differences in material removal rates. Therefore, it is necessary to dynamically adjust the distribution of the reconstructed velocity field, implement deceleration residence in the low curvature region to extend the effective processing time, and restore the reference swing velocity in the high curvature region, thereby achieving a balanced removal rate in the time domain dimension.

Define the polar Angle of a spherical point as θ, The azimuth Angle is β, The swing Angle of the mold is $\theta(t)=\omega_3 t$, The linear velocity of any point $p(\alpha,\beta)$ on the spherical surface is:

$$v_b=\omega_2 R\sin\alpha\cdot\hat{\varphi} \tag{3}$$

The velocity direction is along the tangent line of the latitude ($\hat{\varphi}$ is the unit vector of azimuth). The linear velocity of point Q on the surface of the grinding tool is the superposition of swing and rotation. Among them, the linear velocity of the swing center point O_2 and the tangential rotation velocity relative to C are respectively:

$$v_s=\omega_3 L\left[-\sin\theta\mathbf{y}_1+\cos\theta\hat{\mathbf{z}}_1\right] \tag{4}$$

$$\mathbf{v}_r=\omega_1 r\left[\cos\phi\hat{\mathbf{y}}_2+\sin\phi\hat{\mathbf{z}}_2\right] \tag{5}$$

Here, $\phi=\omega_1 t$ represents the phase Angle of the grinding tool's rotation. When the velocities are combined, we have:

$$\mathbf{v}_t=\mathbf{v}_s+\mathbf{v}_r=\begin{bmatrix}0\\-\omega_3 L\sin\theta+\omega_1 r(\cos\phi\cos\theta-\sin\phi\sin\theta)\\\omega_3 L\cos\theta+\omega_1 r(\cos\phi\sin\theta+\sin\phi\cos\theta)\end{bmatrix} \tag{6}$$

Among them, the relative velocity modulus is

$$v_{rel}=\left\|\mathbf{v}_t-\mathbf{v}_b\right\|=\sqrt{\left(\omega_1 r\cos\phi\right)^2+\left(\omega_3 L+\omega_1 r\sin\phi-\omega_2 R\sin\alpha\right)^2} \tag{7}$$

Contact point p satisfies the position constraint:

$$\|O_1P-O_1O_2\|==\theta+\arcsin\left(\frac{r}{R}\right) \tag{8}$$

Then the speed difference ratio is obtained

$$\frac{v_{rel}^{equator}}{v_{rel}^{polar}}\propto\frac{\omega_3 L+\omega_1 r}{\omega_3 L\sin\alpha}\quad(\alpha\to 0^{\circ}) \tag{9}$$

Among them, $v_{rel}^{equator}$ and v_{rel}^{polar} are divided into the velocities of the equatorial region and the pole region

4. ANALYSIS OF THE DISTRIBUTION TRAJECTORY OF POLISHING ABRASIVE PARTICLES AND SIMULATION ANALYSIS

4.1. Evaluation Method of Polishing Trajectory

Fixed-step trajectory density analysis assesses the uniformity of trajectory distribution by dividing the workpiece surface area along the Z-axis with equal steps, counting the number of trajectory points within each interval, and calculating the ratio of these points to the interval length.

The Voronoi diagram analysis method constructs Voronoi diagrams through discrete point sets, dividing the workpiece surface into multiple regions controlled by abrasive grains. The boundaries of each region are determined by its nearest neighbor abrasive grains, thereby being able to visually reflect the spatial distribution characteristics of abrasive grains. By calculating the area distribution of the Voronoi unit, the local density variation of the abrasive particles can be quantitatively analyzed, and the uniformity of their distribution can be judged.

The macroscopic distribution trend of abrasive particles was quantified by fixed-step trajectory density analysis, and the local density variation and spatial influence range were evaluated by Voronoi diagram analysis method. Combining the two can provide a more comprehensive and accurate analysis of the abrasive distribution, offering strong support for optimizing the abrasive layout.

4.2. Simulation Analysis of Single-Factor Abrasive Particle Parameters

4.2.1. The influence of the initial position of the mold on the uniformity of the motion trajectory

During the spherical polishing process, to ensure uniform polishing of all parts, it is necessary to control the initial swing position of the grinding tool, and its limit range is $\theta = (\theta_L \sim \theta_R)$. Due to the rotation of the ceramic ball, theoretically, taking half of the swing range of the grinding tool can meet the requirement, allowing the abrasive grains to envelop the entire spherical surface. The centerline of the mold does not need to pass through the vertex. It only needs to touch the circle and add a swing at the vertex. When reducing the swing Angle, the rotation Angle is equal to half of the central Angle, defined as θ_m, and the corresponding swing range is θ=(θ_1 to θ_2). Some of the parameters are shown in Tables 1 and 2.

Table 1. Abrasive particle parameters $\theta = 0$

Number	Mold radius r(mm)	The swing Angle of the centerline (β) range	Swing time t (s)
1	6	0 ~ 104.07	21.8
2	8	0 ~ 94.47	20.17
3	10	0 ~ 87.03	18.19
4	12	0 ~ 74.72	15.64

Table 2. Abrasive particle parameters $\theta = \theta_1$

Number	Mold radius r (mm)	The swing Angle of the centerline (β) range	Swing time t (s)
1	6	0 ~ 79.47	16.64
2	8	0 ~ 61.2	12.84
3	10	0 ~ 45.05	9.44
4	12	0 ~ 37.57	7.87

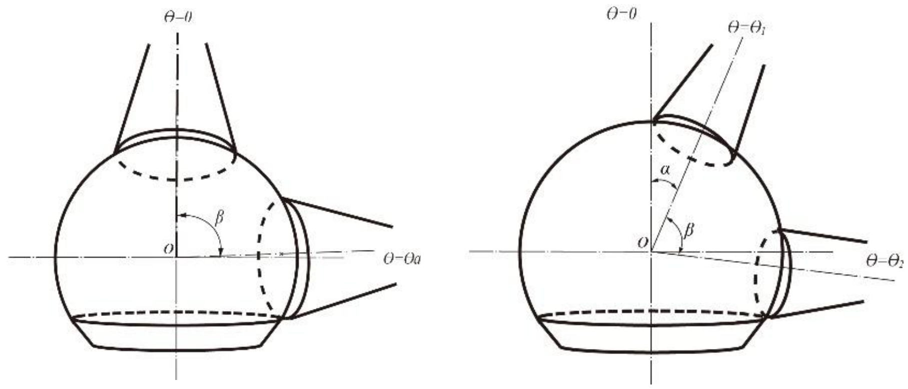

(a) $\theta = 0$ Location (b) $\theta = \theta_1$ Location

Figure 5. Initial position diagram of the mold

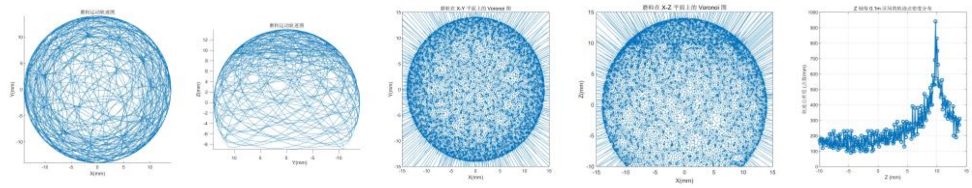

(a) $\theta = 0$

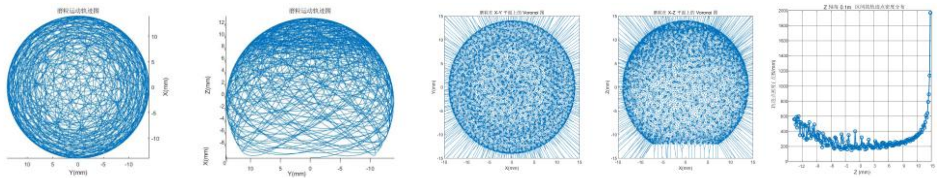

(b) $\theta = \theta_1$

Figure 6. Voronoi diagram of abrasive particle trajectory and analysis of fixed step size

According to the analysis in Figure 6a, it can be observed that when the ceramic ball is close to the top position (with a Z coordinate of 10mm), the trajectory curve is relatively dense and accompanied by more Voronoi division points. This indicates that the polishing amount in this area is significantly higher than that in other parts. With the increase of the Z-axis value, the trajectory density gradually decreases. In the figure, the trajectory densities at both ends are much lower than the peak at Z=10mm. The lower trajectory density indicates insufficient abrasive coverage, which may lead to uneven surface processing of the workpiece, resulting in a rough and uneven surface. Further analysis reveals that the main reason for this situation is that when the grinding tool starts working at the position $\theta = 0$, additional repetitive polishing is carried out in a specific area of the ball head. On the one hand, this area has undergone a normal polishing process. On the other hand, due to the characteristics of the central Angle covered by the grinding tool, this area has endured repeated polishing for an additional half of the central Angle range. In order to optimize the polishing trajectory distribution, the starting point of the grinding tool movement can be redefined by adjusting the initial position, thereby changing the trajectory coverage path. This adjustment can effectively avoid repeated polishing at Z=10mm, and at the same time break the limitation of fixed directionality, making the trajectory distribution more random. In addition, reducing the swing Angle can shorten the movement path of the grinding tool, increase its action time in the effective polishing area, and thereby improve the processing efficiency. Shortening the swing time directly reduces the processing time of a single polishing cycle, allowing the grinding tool to focus on the area that needs to be processed, thereby reducing the phenomenon of local over-polishing and improving the uniformity of the overall polishing quality.

4.2.2. The influence of the grinding tool radius on the uniformity of the motion trajectory

The grinding tool radius, as a key geometric parameter in polishing processing, has an important influence on the uniformity of the processing trajectory and the stability of the material removal distribution. When parameters such as the workpiece rotational speed ω_1, the grinding tool rotational speed ω_2, the grinding tool swing speed ω_3, and the ball head radius R remain unchanged, Taking the grinding tool radii r of different sizes as the research object, the influence of the change of the grinding tool radius r on the uniformity of the abrasive particle movement trajectory is analyzed. Meanwhile, since the swing speed remains constant, Table 2 shows the swing parameters of the abrasive grains with different grinding tool radii.

Table 3. Abrasive particle swing parameters with different grinding tool radii

Number	Mold radius r(mm)	The swing Angle of the centerline (β) range	Swing time t (s)
1	6	0 ~ 79.47	16.64
2	8	0 ~ 61.27	12.84
3	10	0 ~ 45.05	9.44
4	12	0 ~ 37.57	7.87

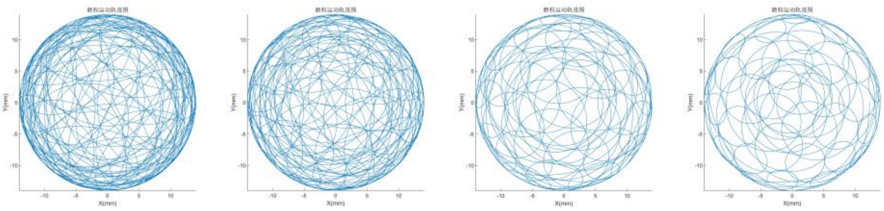

(a) 6mm (b) 8mm (c) 10mm (d) 12mm

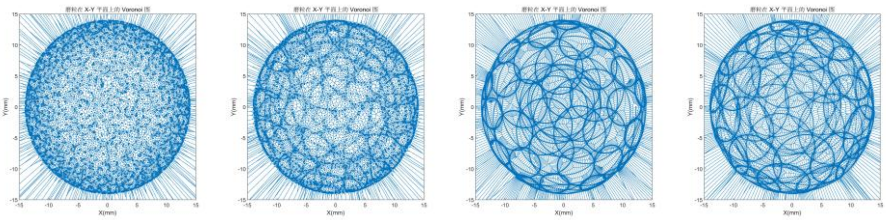

(e) 6mm (f) 8mm (g) 10mm (h) 12mm

Figure 7. The motion trajectories and Voronoi diagrams of the X-Y plane under grinding tools with different radii

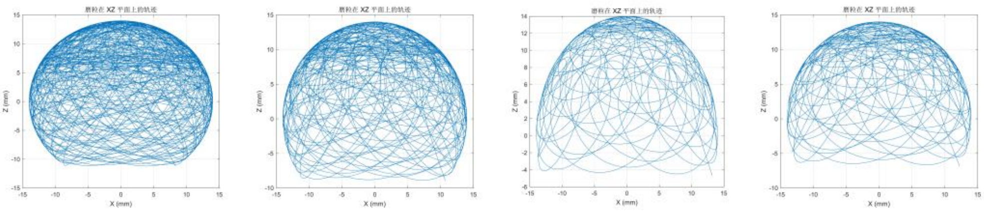

(a) 6mm (b) 8mm (c) 10mm (d) 12mm

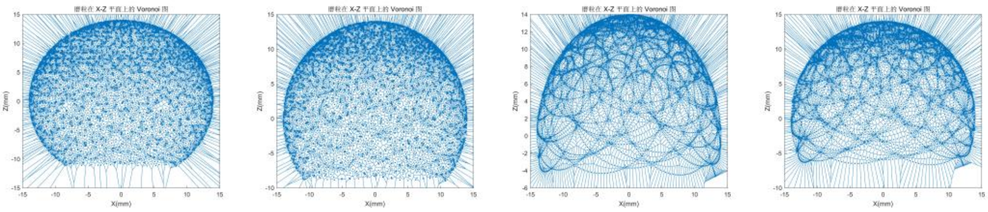

(e) 6mm (f) 8mm (g) 10mm (h) 12mm

Figure 8. The motion trajectories and Voronoi diagrams of the X-Z plane under grinding tools with different radii

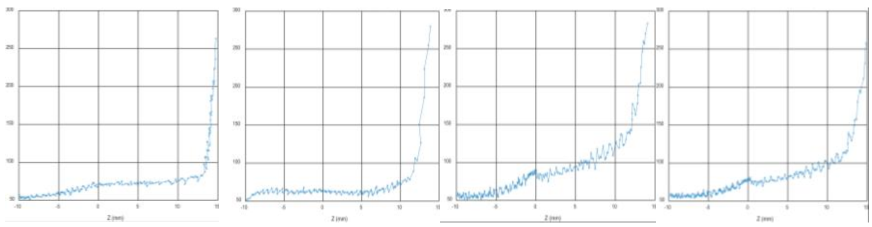

(a) 6mm (b) 8mm (c) 10mm (D) 12mm

Figure 9. Trajectory density maps under grinding tools of different radii

According to the results shown in Figure 9, the density of the trajectory points fluctuates significantly at both ends of the curve, and the degree of fluctuation varies with the radius of the mold. At the beginning of the curve, the density of the trajectory points gradually increases from zero, which is consistent with the trajectory distribution law at the bottom of the ball head. This indicates that the uniformity of the trajectory in this area is poor, which may lead to insufficient coverage or insufficient processing strength. To improve this problem, the swing speed of the mold in this area can be reduced, the action time can be prolonged, and the processing consistency can be enhanced. A sudden increase in density occurs at the termination position of the curve, reflecting that the trajectory distribution at the top of the spherical head is overly concentrated. Appropriately increasing the swing speed can extend the coverage of the trajectory and avoid local accumulation. Furthermore, when the radius of the mold is small, the density of the trajectory points is high but the uniformity decreases. Although increasing the radius reduces the density, it significantly improves the uniformity and makes the processing more stable. Therefore, a smaller radius is beneficial to the local forming quality, while a larger radius can better ensure the overall consistency, optimize the density distribution of trajectory points, and improve the processing stability.

4.2.3. The influence of the grinding tool radius on the uniformity of the motion trajectory

Table 4. The swing parameters of the grinding tool at different rotational speed ratios P

Rotationalspeed ratio P	Grinding tool radius r (mm)	The range of swing angles of the centerline $\beta(^{\circ})$	Swing time t (s)
2	10	0 ~ 45.05	9.44
7	10	0 ~ 45.05	9.44
11	10	0 ~ 45.05	9.44
2.3	10	0 ~ 45.05	9.44
7.3	10	0 ~ 45.05	9.44
11.3	10	0 ~ 45.05	9.44
$\sqrt{2}$	10	0 ~ 45.05	9.44
$\sqrt{5}$	10	0 ~ 45.05	9.44
$\sqrt{7}$	10	0 ~ 45.05	9.44
$\sqrt{11}$	10	0 ~ 45.05	9.44

Using the method of selecting control variables as mentioned above, when the swing center line of the initial position of the grinding tool is located at θ_1, and the parameters such as the fixed workpiece rotational speed ω_1, the grinding tool swing speed ω_3, and the grinding tool radius r remain unchanged, the influence of the rotational speed ratio $p = \omega_1 / \omega_2$ on the uniformity of the abrasive particle movement trajectory is explored. Select different grinding tool rotational speeds ω_2 and observe the influence of different rotational speed ratios P on the uniformity of the abrasive particle movement trajectory. Observe the movement of the grinding tool for one cycle and the influence of the rotational speed ratio on the trajectory of the abrasive grains on the ball surface. Table 4 shows the swing parameters of the grinding tool at different rotational speed ratios P.

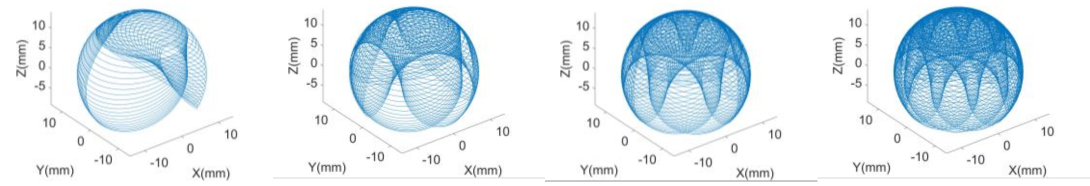

(a) p=2 (b) p=5 (c) p=7 (d) p=11

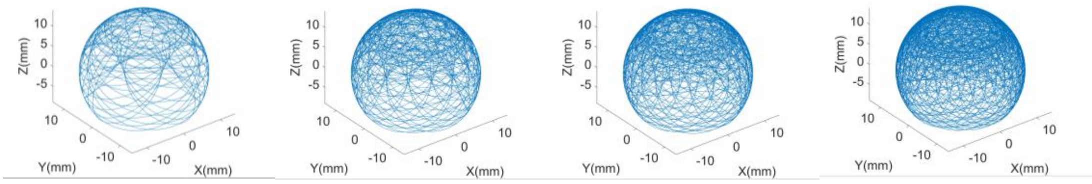

(e) p= $2.\dot{3}$ (f) p= $5.\dot{3}$ (g) p= $7.\dot{3}$ (h) p= $11.\dot{3}$

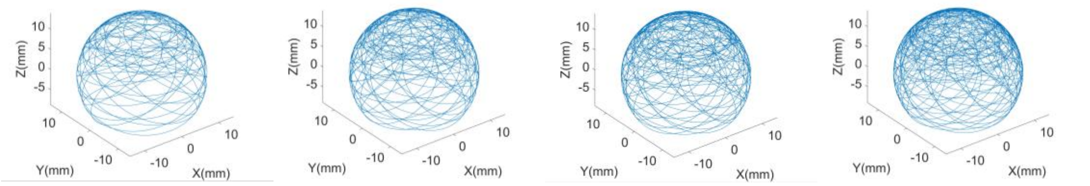

(e) p= $\sqrt{2}$ (f) p= $\sqrt{5}$ (g) p= $\sqrt{7}$ (h) p= $\sqrt{11}$

Figure 10. Abrasive particle trajectory diagrams under different rotational speed ratios

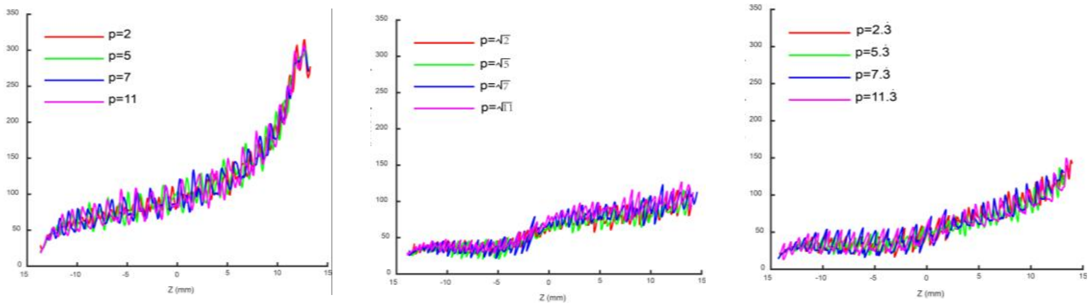

(a) nteger. (b) infinite recurring decimal (c) infinite non-recurring decimal

Figure 11. Trajectory density maps at different rotational speed ratios P

It can be known from Figure 10 that compared with the integer specific rotational speed, the abrasive trajectory of the non-integer specific rotational speed is denser, and the uniformity of the abrasive polishing forming quality on the ball surface is better. Compared with the integer rotational speed ratio, the non-integer rotational speed ratio can break the periodic law of the trajectory, making the movement trajectory of the abrasive grains present a more complex and random distribution on the workpiece surface. This randomness effectively avoids the repetitive covering of trajectories, enhances the density and uniformity of trajectories on the spherical surface, thereby ensuring the uniformity of surface quality during the processing. Further quantitative analysis through Figure 11 shows that from the overall trend, as p changes from an integer to a finite recurring decimal and then to an infinite non-recurring decimal, the uniformity and complexity of the trajectory gradually increase. The integer ratio leads to overly regular trajectories and severe repetitive coverage. However, the finite cyclic decimal ratio can partially alleviate this problem, but there is still a certain regularity. The trajectory distribution with an infinite non-cyclic fractional ratio is close to complete randomization, achieving the best processing quality.

4.2.4. The influence of uniform pendulum speed and variable pendulum speed on the uniformity of the motion trajectory

Select the control variable and change the swing speed of the mold. According to Equation (1.9), it can be known that due to the difference in curvature, the linear velocities at different points on the spherical surface are different. The surface of the sphere is respectively divided into three regions: the near-polar region, the transition region and the equatorial region, as shown in Figure 12. When the swing center line of the initial position of the grinding tool is located at θ_1, and the parameters such as the rotational speed ω_1 of the fixed workpiece, the rotational speed ω_2 of the grinding tool, and the radius r of the grinding tool remain unchanged, the influence of the uniform variation of the rotational speed ratio and the swing speed on the uniformity of the abrasive particle movement trajectory is explored. According to Equation (1.9), it can be known that due to the influence of different linear velocities, the pendulum velocities distributed in each region also have certain differences. Observe the movement of the grinding tool for one cycle and the influence of the pendulum speed on the trajectory of the abrasive grains on the ball surface. Table 5 shows the polishing parameters of the grinding tool at different pendulum speeds.

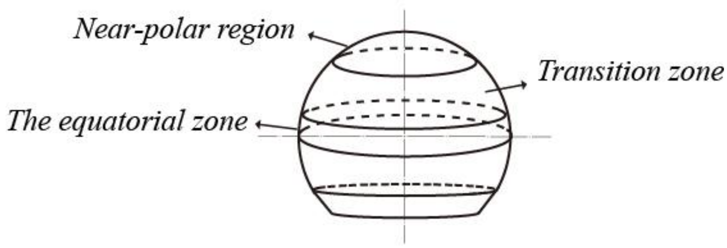

Figure 12. The division diagram of the surface area of the sphere

Table 5. The ratio of pendulum speeds in different regions

Region	Swing Angle β range	Range of polar Angle A	speed ratio
Near-polar region	$\beta \le 10^{o}$	$0 < \beta \le 25^{o}$	2.5-3
Transition zone	$10^{o} < \beta \le 25^{o}$	$25^{o} < \beta \le 65^{o}$	1.2-1.5
The equatorial zone	$25^{o} < \beta \le 35^{o}$	$65^{o} < \beta \le 90^{o}$	1

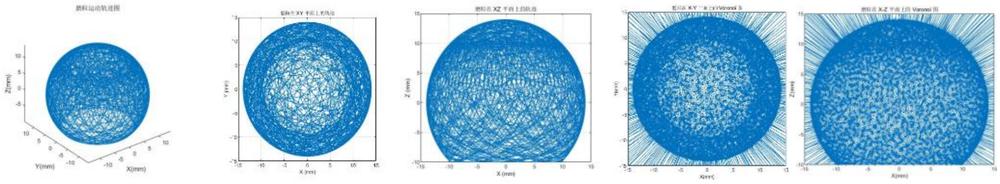

Figure 13. The motion trajectory and Voronoi diagram under uniform pendulum velocity

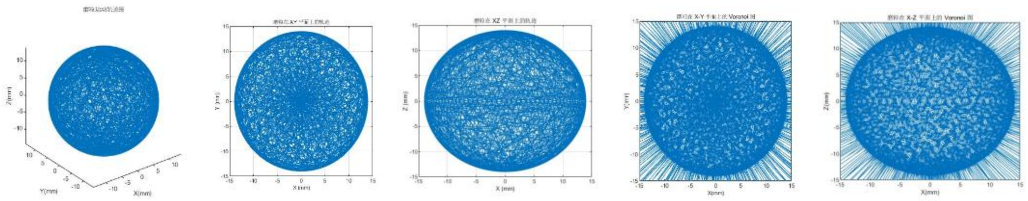

Figure 14. The planar motion trajectory and Voronoi diagram under uniform pendulum velocity

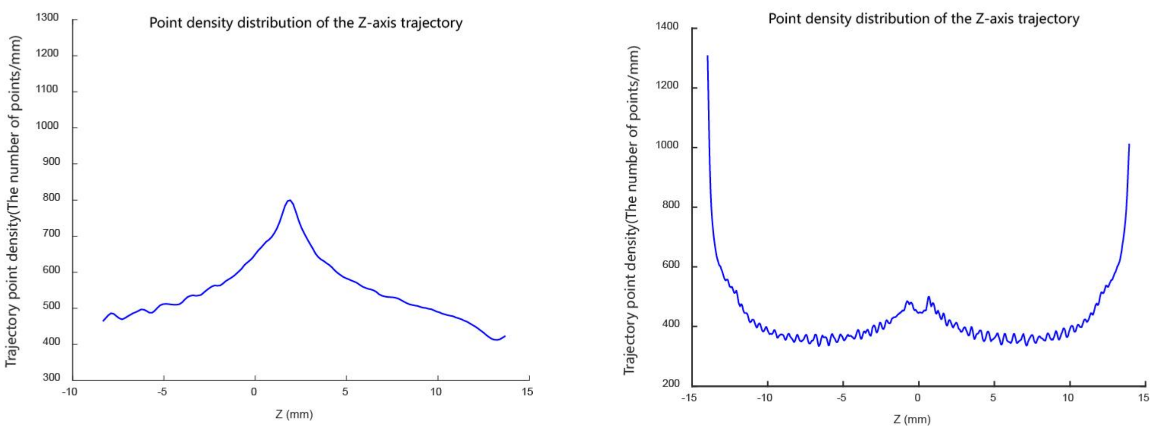

(a) Uniform trajectory density map (b) Variable speed trajectory density map

Figure 15. Trajectory density map under uniform variation and uniform pendulum velocity

It can be seen from the experimental results shown in Figure 14 that during the uniform swing process, the passing frequency of the abrasive particles in the same area shows a significant decreasing trend, thereby forming a sparse spiral trajectory. Especially in the near-pole region, with the increase of the pole Angle, the linear velocity of the contact point of the grinding tool shows the characteristic of linear attenuation. When the polar Angle approaches the limit, the linear velocity at the contact point of the mold almost drops to the lowest level, resulting in the trajectory density in this area being only about 45% to 55% of that in the equatorial area, as shown in Figure 15-a. This phenomenon indicates that as the polar region approaches, the contact effect between the mold and the sphere significantly weakens, and the distribution of the trajectory becomes sparse. Furthermore, due to the difference in the kinematic coupling direction, the velocity direction in the polar region is relatively single. In this area, the Angle between the rotation axis of the grinding tool and the tangent direction of the swing trajectory is close to zero, making the vector motion of the abrasive grains almost completely collinear. This leads to an increase in the repeatability of the trajectory, but the range of the trajectory is relatively narrow. Therefore, the polishing effect in the polar region is relatively limited, and the trajectory density further decreases. In the transition zone and the equatorial zone, due to the certain dynamic included Angle between the rotation and swing velocity directions of the grinding tool, a cross-cutting effect occurs. This effect significantly increases the frequency of contact between the mold and the surface of the sphere, thereby causing the trajectory density to reach its peak in these areas. This phenomenon indicates that in the transition zone and the equator zone, due to the synergistic effect of the two motion modes, the grinding effect has been effectively enhanced, the trajectory is denser, and the uniformity is better. To further optimize the polishing effect, in the experiment, by dynamically adjusting the swing speed, the swing speed in the near-pole region was adjusted, and the polishing dwell time in this area was appropriately increased. As shown in Figures 14 and 15-b, after adjustment, the trajectory density in the near-pole region has been significantly improved by 40%. This adjustment not only effectively improves the trajectory distribution in the near-pole region, but also enhances the uniformity and efficiency of the entire polishing process.

5. EXPERIMENTAL VERIFICATION OF THE TEXTURED MODEL

In order to verify the proposed polishing trajectory model, polishing experiments were conducted on the polishing workbench for verification. In order to obtain clear trajectory patterns on the surface of ceramic balls. Select the corresponding parameters for polishing verification, as shown in Table 6 specifically

This experiment adopts the grinding processing method. The workpiece rotates at a rotational speed of 755r/min, while the grinding tool performs compound motion at a high rotational speed of 2000r/min and a pendulum speed of 13r/min, and is continuously subjected to a pressure of 30N for 15 minutes. Efficient grinding is achieved through the speed difference between the workpiece and the grinding tool. The swing speed ensures the uniformity of grinding. Constant pressure and time control the amount of material removed. Finally, the surface quality after processing or the performance of the grinding tool is evaluated.

Table 6. Experimental Parameter Table

Experimental parameters	Numerical value
Rotational speed (workpiece)	755r/min
Rotational speed (mold)	2000r/min
Pendulum speed (mold reference)	13r/min
Pressure	30N
Time	15min

The polished texture and the simulated texture in the experiment are shown in Figure 16. It can be seen from this that the simulated grinding texture is consistent with the grinding texture obtained in the experiment.

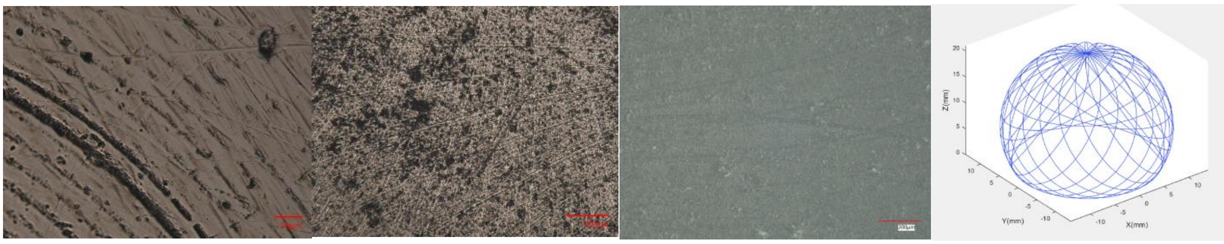

Figure 16. The trajectory morphology obtained by polishing and its simulation results

6. CONCLUSIONS

(1) By constructing a three-dimensional kinematic model of abrasive grains and analyzing the influence of polishing process parameters on the abrasive grain trajectory, it was found that optimizing the initial position, radius and rotational speed ratio could significantly improve the uniformity of material removal and surface quality. The experiment verified the validity of the simulation model

(2) Research shows that reducing the swing Angle of the grinding tool and increasing the residence time in a specific area can improve the trajectory density in the near-pole zone and avoid local excessive polishing. The application of non-integer rotational speed ratios makes the abrasive particle distribution more random and improves the uniformity of surface quality.

(3) By combining the fixed step size analysis method and the Voronoi diagram analysis method, the abrasive particle trajectories were quantitatively evaluated, and the effectiveness of the optimized trajectories was verified through actual polishing experiments. The results show that the optimized trajectory significantly reduces the surface roughness and improves the processing efficiency and consistency.

REFERENCES

[1] Wu Zhengjiang, Yan Wei, Su Yunfeng, et al. Research Progress of High-Performance Ceramic Lubricating Materials [J]. Journal of Tribology, 2025: 30.

[2] Liu Junwei, Fang Jie, Fan Caihe, et al. Preparation Principle and Current Situation of three-dimensional Network Structure Ceramic-reinforced Metal Matrix Composites [J]. Chinese Journal of Nonferrous Metals, 2025: 34.

[3] Yi Chuantong. Development of Special Mixed Abrasive Fluid for Precision Grinding of Silicon Nitride Ceramic Balls [D/OL] Shenyang Jianzhu University, [2025] [April 20, 2025]

[4] Zhu Congrong, Lyu Binghai, Yuan Julong. Research on the Chemical Mechanical Polishing Mechanism of Silicon Nitride Ceramic Balls [J]. China Mechanical Engineering, 2010, 21(10): 1245-1249.

[5] Yang Tiebin, Wang Liqin, Guyue, et al. Research on Surface Defects of Precision Machining of Silicon Nitride Ceramic Balls [J]. Lubrication & Sealing, 2006(7): 45-47, 70.

[6] Li Fei, Chen Shulin, Cui Pangbo, et al. Optimization of Abrasive Belt Grinding Trajectory for Integral Bladed Disk Robot and Its Experiment [J/OL]. Diamond & Abrasives Engineering, 2022, 42(1): 23-29.

[7] Wang Huan, Ding Derui, Wang Yongxiong. An Algorithm for Grinding operation Planning of orthopedic robots [J]. Computer Simulation, 2019, 36(5): 354-359.

[8] Zhang Dezheng, Wang Buyun, Yang Ou, et al. Research on Multi-axis Cooperative Motion Control of Omnidirectional Heavy-duty AGV [J/OL]. Computer Measurement & Control, 2022, 30(4): 91-97.

[9] Wang Zhihui, Gu Zhipeng, Yang Tao. Research on the Removal Mechanism of Polishing Materials Assisted by Ultrasonic Vibration [J]. Machinery Manufacturing, 2023, 61(8): 69-72.

[10] Fan Dengsheng. Simulation Analysis of Magnetic Field Characteristics in Magnetic Grinding and Polishing of Parts Surfaces [J/OL] Mechanical Research and Application, 2024, 37(3): 27-30.

[11] Ni Yongsen, Zhang Lei, Chen Hengxuan, et al. Numerical Simulation Research on the Trajectory Characteristics of Bionic Waterfowl entering the Water [J/OL]. China Shipbuilding Industry, 2025.

[12] Wang Chengbing, Li Haibin, Jiang Lei, et al. Research on the Grinding Wheel Grinding Trajectory Algorithm of the Chip Separation Groove of the Peripheral Teeth of End Mills [J]. Tool Technology, 2022, 56(4): 70-74.

[13] Zha Tijian, Xu Liming, Luo Rui, et al. Research on the Wear of High-hardness Spherical Grinding Wheels Ground by Cup-shaped Grinding Wheels [J/OL]. Tool Technology, 2013, 47(2): 3-7.

[14] Wang Yujue, Xu Liming, Li Dongdong, et al. Texture analysis of oscillating spherical grinding Surfaces [J/OL]. Journal of Shanghai Jiao Tong University, 2012, 46(5): 740-745.